*Pedosphere* **16**(6): 681–689, 2006
ISSN 1002-0160/CN 32-1315/P

Published by Elsevier Limited and Science Press

PEDOSPHERE

www.elsevier.com/locate/pedosphere

# Impacts of Land Use and Cover Change on Land Surface Temperature in the Zhujiang Delta*[1]

QIAN Le-Xiang[1,2], CUI Hai-Shan[1] and CHANG Jie[2,3]

[1] *School of Geographical Sciences, Guangzhou University, Guangzhou 510006 (China). E-mail: lxqian@henu.edu.cn*
[2] *College of Environment & Planning, Henan University, Kaifeng 475004 (China)*
[3] *Program in Geographic Information Sciences, University of Texas at Dallas, Richardson, TX 75083 (USA)*

(Received March 8, 2006; revised July 19, 2006)

## ABSTRACT

Remote sensing and geographic information systems (GIS) technologies were used to detect land use/cover changes (LUCC) and to assess their impacts on land surface temperature (LST) in the Zhujiang Delta. Multi-temporal Landsat TM and Landsat ETM+ data were employed to identify patterns of LUCC as well as to quantify urban expansion and the associated decrease of vegetation cover. The thermal infrared bands of the data were used to retrieve LST. The results revealed a strong and uneven urban growth, which caused LST to raise 4.56 °C in the newly urbanized part of the study area. Overall, remote sensing and GIS technologies were effective approaches for monitoring and analyzing urban growth patterns and evaluating their impacts on LST.

*Key Words*: land surface temperature, land use/cover change, Landsat ETM+, Landsat TM, Zhujiang Delta

## INTRODUCTION

Reflecting the biophysical state of the earth's surface, land use and land cover serve as a fundamental interface of energy and matter exchange between the geosphere and biosphere. Changes in land use/cover affect the underlying biotic diversity, actual and potential primary productivity, soil quality, runoff, and sedimentation rates (Hu *et al.*, 2004), the dynamics of which can not be well understood without knowledge of the land use/cover change (LUCC) that drives them. LUCC has environmental implications at local and regional levels and is linked even to environmental processes at the global level. Because of the interrelated nature among different environmental elements, the direct impact on one element may cause indirect influence on others.

Research on land surface temperature (LST) shows that the partitioning of sensible and latent heat fluxes is a function of varying surface soil water content and vegetation cover (Owen *et al.*, 1998), causing various responses in the resulting surface radiant temperature. A higher level of latent heat exchange is often found in more vegetated areas, whereas sparsely vegetated areas, such as urban districts, favor sensible heat exchange (Oke, 1982). Urbanization has been a major force of LUCC throughout human history that has had a great impact on climate change (Gao *et al.*, 2003). Covered with buildings, roads, and other impervious surfaces, urban areas generally have higher absorption of solar radiation and greater thermal capacity and conductivity (Zhou, 2006), leading to a relatively higher temperature in the urban areas compared with the surrounding rural areas (Zhou *et al.*, 2005; Zhou, 2006).

Alteration of the earth's surface from LUCC can be dramatic. This is especially true during a period of rapid urban development, because large amounts of natural vegetation are being removed and replaced by impervious surfaces, such as metal, asphalt, and concrete during the process. This alteration will inevitably result in the redistribution of responses to the incoming solar radiation and

*[1]Project supported by the Science and Technology Project Foundation of Guangzhou (No. 2005Z3-D0551) and the Science and Technology Project Foundation of Guangzhou Education Bureau (No. 62026).

cause amplification of the contrast in surface radiance and air temperature between rural and urban areas. The resulting difference in ambient temperature between the urban and its surrounding rural area, in conjunction with the waste heat released from urban residences, transportation, and industry, is referred to as the urban heat island (UHI) effect. The temperature differences between the urban and the rural areas were usually modest, averaging less than 1 °C, but occasionally, rising to several degrees when topographical and meteorological conditions are favorable for a UHI to develop.

Studies on LST characteristics of urban areas using satellite remote sensing data have been conducted primarily using the National Oceanic and Atmospheric Administration's (NOAA) advanced very high resolution radiometer (AVHRR) data (Kidder and Wu, 1987; Balling and Brazell, 1988; Roth *et al.*, 1989; Gallo *et al.*, 1993). However, the 1.1 km spatial resolution of these data was found suitable only for mapping temperature at the regional level. Although there were several applications utilizing only the brightness temperature at the satellite level (Mansor *et al.*, 1994; Saraf *et al.*, 1995; Zhang *et al.*, 1997) or just the digital number (DN) value (Ritchie *et al.*, 1990; Oppenheimer, 1997) of the thermal infrared band, Landsat TM thermal infrared data with a much higher spatial resolution of 120 m have seldom been used to derive LST. Only a few researchers have practically derived real LST from Landsat TM thermal data (Hurtado *et al.*, 1996; Sospedra *et al.*, 1998), but there was no mention of employing Landsat ETM+ thermal infrared data (60 m spatial resolution) in the literature.

Up to now, no attempt has been made to study LUCC or urban expansion-induced LST change over time at a local level using multi-date Landsat thermal infrared data. This situation was ascribed to the inherent weakness of Landsat data, such as no real-time calibration and low repeat cycles. The lack of a simple and suitable algorithm to retrieve LST from the Landsat thermal infrared band has also contributed to the fact that the Landsat thermal infrared data have rarely been used in LST related applications. Qin and Karnieli (2001) developed a new computational efficient algorithm to retrieve LST from Landsat TM thermal data based on a thermal radiance transfer equation and achieved high estimation accuracy. In the algorithm impacts from both the atmosphere and the emitted ground on the thermal radiance transfer model are directly taken into consideration by including three essential parameters for retrieval: emissivity, transmittance, and effective mean atmospheric temperature.

Since the adoption of economic reform policies in 1978 and the accelerated economic development in China, land use/cover has undergone a tremendous change. Rapid urban growth has exerted great pressure on China's environment (Pan and Zhao, 2005). This is particularly true in the coastal regions such as the Zhujiang Delta, where massive areas of agricultural land are disappearing each year, giving way to urban or related uses. In addition, the lack of appropriate land use planning and strategies for sustainable development has exacerbated the environment and caused severe consequences. Therefore, evaluating the magnitude and pattern of urban growth and assessing the impact of rapid urban expansion on the environment have become an urgent need. These constitute the purpose of this study. Specifically, the objectives were to examine urban growth in the Zhujiang Delta region and analyze its impact on LST using remote sensing and GIS technologies.

## MATERIALS AND METHODS

### *Study site*

The Zhujiang Delta is located between latitudes 21° 30′ and 23° 45′ N, and longitudes 112° 00′ and 115° 25′ E. It is the third biggest river delta in China with an area of 41 698 km$^2$. The study area focused on the central part of the Zhujiang Delta with a length of 90 km from east to west and a width of 40 km from north to south, where was completely covered with satellite data.

The Zhujiang Delta is one of the largest metropolises with the highest concentration of economic activities in South China, within which mega-cities such Guangzhou (China's sixth largest city), Hong Kong, and Macao are situated. The establishment of the Shenzhen and Zhuhai Special Economic Zones in 1979 and Zhujiang Delta Economic Open Zone in 1985 within the study area has attracted enormous

investment from Hong Kong, Macao, and foreign countries. As a result, many manufacturing factories have been established in the region in the form of village-township enterprises, most of which are labor-intensive industries, associated with the production of seafood, poultry, vegetables, fruit and flowers, *etc.* The dramatic economic expansion has set the economy of the delta as a model for China's regional development (Lo, 1989; Weng, 1998). The rapid economic development, however, has brought about significant changes in land use/cover patterns, bearing considerable impacts on the LST of the region.

*LST and LUCC from satellite data*

Because of the unavailability of the *in situ* atmospheric characteristic data during the pass of the satellite in this study, a 'mono-window algorithm' was adopted to retrieve the LST from the Landsat thermal infrared band (Qin and Karnieli, 2001; Qin *et al.*, 2001, 2003) so as to detect the changes of LST between 1990 and 2000.

Landsat TM and ETM+ data acquired on October 13, 1990 and September 14, 2000, respectively, were employed in this study. Each scene of Landsat images was enhanced using the histogram equalization approach to gain a higher contrast of the images (Wu *et al.*, 2004), so ground control points could be easily identified for the purpose of geometric rectification. All images were rectified to a common Universal Transverse Mercator coordinate system based on the 1:50 000 topographic maps of Guangdong Province. Each image was then radiometrically corrected using a relative radiometric correction method. A supervised classification with the maximum likelihood algorithm was conducted to classify the Landsat images using bands 2 (green), 3 (red), and 4 (near-infrared).

To derive the land use/cover maps for years 1990 and 2000, seven land use/cover types were used in the study, including urban or built-up land, barren land, cropland, horticulture farms, dike-pond land, forest, and water body. The accuracy of the classification was verified with *in situ* ground reference information or with the existing land use/cover maps that have been field-verified. To document LUCC, a cross-tabulation change detection method was employed, which produced a change matrix in which the quantities of the overall LUCC as well as gains and losses in each land use/cover category between 1990 and 2000 were calculated.

*Analysis*

To specifically analyze urban land change in terms of the nature, rate, and distribution of the urban expansion, images of urban and built-up land were extracted from their original land use/cover classification maps. The extracted areas of urban land use/cover types were then overlaid and recoded to obtain an urban land change (expansion) image.

The radiometrically corrected Landsat TM and ETM+ thermal infrared data were employed to derive land surface temperatures of the two study years. According to Qin and Karnieli (2001), the LST ($T_s$, K) can be computed from Landsat TM and ETM+ thermal infrared data as follows:

$$T_s = \{a_6 \times (1 - C_6 - D_6) + [b_6 \times (1 - C_6 - D_6) + C_6 + D_6] \times T_6 - D_6 \times T_a\}/C_6 \quad (1)$$

where $a_6$ and $b_6$ are constants, generally being $-67.355351$ and $0.458606$, respectively; $C_6$ and $D_6$ are the intermediate variables, which can be calculated by Eqs. 2 and 3; $T_6$ is the brightness temperature integrated over TM and ETM+ thermal band in K and can be obtained by Eq. 4, which is similar to Planck's radiance function; and $T_a$ is atmospheric average temperature in K:

$$C_6 = \varepsilon_6 \tau_6 \quad (2)$$

$$D_6 = (1 - \varepsilon_6)[1 + (1 - \varepsilon_6)\tau_6] \quad (3)$$

where $\varepsilon_6$ is emissivity and $\tau_6$ is transmittance, and

$$T_6 = K_2 / \ln(K_1/R + 1) \quad (4)$$

where $R$ is the blackbody spectral radiance for temperature and $K_1$ and $K_2$ are constants with $K_1 = 607.76\ \mathrm{Wm^{-2}\ sr^{-1}\ \mu m^{-1}}$ and $K_2 = 1\,260.56$ K for TM onboard Landsat-5 (Sospedra *et al.*, 1998); whereas $K_1 = 666.09\ \mathrm{Wm^{-2}\ sr^{-1}\ \mu m^{-1}}$ and $K_2 = 1\,282.71$ K for ETM+ onboard Landsat-7.

Therefore, in order to calculate the real LST value for each cell on an image using Eq. 1, three essential parameters $T_a$, $\tau_6$, and $\varepsilon_6$ were needed. In the Zhujiang Delta, $T_a$, $\tau_6$, and $\varepsilon_6$ were obtained using Eqs. 5, 6, and 7a–7c:

$$T_a = 16.011 + 0.92621T_0 \tag{5}$$

$$\tau_6 = 1.031412 - 0.11536\omega \tag{6}$$

$$\varepsilon_6 = 0.958942 + 0.0898322P_v - 0.067158P_v^2 \quad (P_v < 0.5) \tag{7a}$$

$$\varepsilon_6 = 0.960842 + 0.0860322P_v - 0.067158P_v^2 \quad (P_v = 0.5) \tag{7b}$$

$$\varepsilon_6 = 0.962642 + 0.0822322P_v - 0.067158P_v^2 \quad (P_v > 0.5) \tag{7c}$$

where $T_0$ is the air temperature near the ground; $\omega$ stands for moisture content, having a value of 1.6–3.0 g $\mathrm{cm^{-2}}$ in the study area, and $P_v$ is the fractional coefficient of vegetation coverage, which can be derived from the normalized difference vegetation index (NDVI) values with the following equation:

$$P_v = (\mathrm{NDVI} - \mathrm{NDVI_1})/(\mathrm{NDVI_2} - \mathrm{NDVI_1}) \tag{8}$$

where $\mathrm{NDVI_1}$ is the minimum value of the NDVI for bare soil over the region of interest and $\mathrm{NDVI_2}$ is the highest NDVI expected for a fully vegetated pixel. Because the absolute values of NDVI tended to vary temporally in a non-systematic manner over the years, the fractional coefficients of vegetation coverage ($P_v$) of each year were calculated according to Eq. 8 to obtain the scaled NDVI values. Image differencing was then performed between $P_v$ images of 1990 and 2000.

With all the above equations, the LST from the Landsat TM and ETM+ data were retrieved. In order to understand the impacts of LUCC on the thermal characteristics of various land surfaces, the average LST of each land use/cover type in 1990 and 2000 were calculated with their standard deviations.

The resultant LST ($T_s$) images could then be used to produce an image of LST change between 1990 and 2000 using the image-differencing operator. With a similar approach and based on the derived NDVI images and land use/cover maps of 1990 and 2000, images reflecting the changes of NDVI and land use/cover patterns between the two years could also be produced. The comparison of change in LST with that in land use/cover patterns and with that in NDVI provided an opportunity to analyze the relationships among these changes. The relationship between LST and NDVI was investigated for each land cover type through Pearson's correlation analysis at the pixel level. The significance of each correlation coefficient was determined using a one-tail student's $t$-test.

## RESULTS AND DISCUSSION

The overall accuracy of the land use/cover map for 1990 and 2000 is shown in Tables I and II. Their corresponding kappa indices were 0.8973 and 0.9178. The maximum likelihood classification delivered reasonably high overall accuracies and acceptable producer's and user's accuracies for most classes in both years. This was sufficiently good for change detection analysis so that spurious urban growth, being detected as a result of misclassification, could be avoided.

Table III showed that there has been considerable LUCC for the study area in the Zhujiang Delta from 1990 to 2000. Urban or built-up land, horticulture farms, and dike-pond land types have increased, whereas barren land, cropland, forest, and water types have decreased.

A detail comparison of the 1990 and 2000 land use/cover map further indicated that the increase in urban or built-up land (57.8%) was primarily from the loss of forest (29.5%) and cropland (12.5%); the increase in horticulture farm (32.5%) was mainly from the decreases in forest (64.4%) and cropland

TABLE I

Error matrix of the land use/cover mapping for the Zhujiang Delta in 1990

| Land use/cover[a)] | Reference data | | | | | | | | RT[b)] | CT[b)] | NC[b)] | PA[b)] | UA[b)] | OA[b)] |
|---|---|---|---|---|---|---|---|---|---|---|---|---|---|---|
| | UC | UB | BL | CR | HF | DP | FO | WB | | | | | | |
| | | | | | | | | | | | | % | | |
| UC | 0 | 0 | 0 | 0 | 0 | 0 | 0 | 0 | 0 | 0 | 0 | - | - | 93.0 |
| UB | 0 | 21 | 0 | 0 | 0 | 0 | 0 | 0 | 21 | 21 | 21 | 100.0 | 98.0 | |
| BL | 0 | 0 | 1 | 0 | 0 | 0 | 0 | 0 | 1 | 1 | 1 | 100.0 | 100.0 | |
| CR | 0 | 0 | 0 | 45 | 4 | 0 | 0 | 0 | 47 | 49 | 45 | 95.7 | 91.8 | |
| HF | 0 | 0 | 0 | 0 | 7 | 0 | 3 | 0 | 20 | 10 | 7 | 35.0 | 70.0 | |
| DP | 0 | 0 | 0 | 0 | 0 | 18 | 0 | 0 | 18 | 18 | 18 | 100.0 | 100.0 | |
| FO | 0 | 0 | 0 | 2 | 9 | 0 | 123 | 0 | 126 | 134 | 123 | 97.6 | 91.8 | |
| WB | 0 | 0 | 0 | 0 | 0 | 0 | 0 | 23 | 23 | 23 | 23 | 100.0 | 100.0 | |

[a)]UC = unclassified; UB = urban or built-up land; BL = barren land; CR = cropland; HF = horticulture farm; DP = dike-pond land; FO = forest; and WB = water body.
[b)]RT = reference totals; CT = classified totals; NC = number correct; PA = producer's accuracy; UA = user's accuracy; and OA = overall accuracy.

TABLE II

Error matrix of the land use/cover mapping for the Zhujiang Delta in 2000

| Land use/cover[a)] | Reference data | | | | | | | | RT[b)] | CT[b)] | NC[b)] | PA[b)] | UA[b)] | OA[b)] |
|---|---|---|---|---|---|---|---|---|---|---|---|---|---|---|
| | UC | UB | BL | CR | HF | DP | FO | WB | | | | | | |
| | | | | | | | | | | | | % | | |
| UC | 0 | 0 | 0 | 0 | 0 | 0 | 1 | 0 | 0 | 1 | 0 | - | - | 93.4 |
| UB | 0 | 48 | 0 | 0 | 0 | 0 | 1 | 0 | 48 | 49 | 48 | 100.0 | 98.0 | |
| BL | 0 | 0 | 5 | 0 | 0 | 0 | 0 | 0 | 5 | 5 | 5 | 100.0 | 100.0 | |
| CR | 0 | 0 | 0 | 59 | 5 | 0 | 0 | 0 | 64 | 64 | 59 | 92.2 | 92.2 | |
| HF | 0 | 0 | 0 | 5 | 44 | 0 | 2 | 0 | 52 | 51 | 44 | 84.6 | 86.3 | |
| DP | 0 | 0 | 0 | 0 | 0 | 11 | 0 | 0 | 11 | 11 | 11 | 100.0 | 100.0 | |
| FO | 0 | 0 | 0 | 0 | 3 | 0 | 50 | 0 | 54 | 53 | 50 | 92.6 | 94.3 | |
| WB | 0 | 0 | 0 | 0 | 0 | 0 | 0 | 22 | 22 | 22 | 22 | 100.0 | 100.0 | |

[a)]UC = unclassified; UB = urban or built-up land; BL = barren land; CR = cropland; HF = horticulture farm; DP = dike-pond land; FO = forest; and WB = water body.
[b)]RT = reference totals; CT = classified totals; NC = number correct; PA = producer's accuracy; UA = user's accuracy; and OA = overall accuracy.

(24.7%); and the increase in dike-pond land (21.9%) mostly came from forest (35.8%) and cropland (21.4%), too. On the other hand, the decrease in barren land (67.0%) was mostly transformed to forest (50.4%) and cropland (26.6%); the decrease in cropland (11.4%) largely contributed to the increase of forest (52.1%) and urban or built-up land (5.7%); and the decrease in forest (10.8%) became the increase in cropland (23.7%), the horticulture farm (4.8%), and urban or built-up land (3.4%).

The actual areal extent and spatial occurrence of urban expansion revealed that the urban expansion in the study area took place primarily in Nanhai, Shunde, Foshan (near the old Baiyun Airport), and part districts of Guangzhou, such as Tianhe, Huangpu, and the southeast of Haizhu. Massive urban sprawl in these areas, due to urbanization of originally rural areas, has been a common phenomenon in recent years of China. A distinct pattern of rapid urban expansion was primarily observed along the highway connecting Guangzhou, Dongguan, Shenzhen, and Hong Kong, where a great many manufacturing plants and associated housing units built by investors from Hong Kong were concentrated.

The average LST of each land use/cover type in 1990 and 2000 (Table IV) showed that urban or built-up land exhibited the highest LST for both years. This implied that urban development, due to the replacing of natural vegetation with non-evaporating, non-transpiring surfaces, such as stone, metal,

TABLE III

Land use/cover change matrix in the Zhujiang Delta from 1990 to 2000

| Land use/cover[a)] | UC[b)] | Urban land | Barren land | Crop-land | HF[b)] | Dike-pond | Forest | Water body | Total area in 1990 |
|---|---|---|---|---|---|---|---|---|---|
| | ha | | | | | | | | |
| UC | 1833 | 0 | 0 | 0 | 0 | 0 | 0 | 0 | 1833 |
| Urban land | 0 | 26706 | 92 | 3878 | 127 | 2417 | 5190 | 1480 | 39890 |
| Barren land | 0 | 937 | 43 | 1557 | 72 | 202 | 1605 | 211 | 4627 |
| Cropland | 0 | 7858 | 407 | 19947 | 4171 | 4627 | 36016 | 3169 | 76195 |
| HF | 0 | 780 | 34 | 2384 | 1306 | 476 | 7351 | 423 | 12754 |
| Dike-pond | 0 | 4007 | 113 | 2064 | 121 | 4565 | 4982 | 1893 | 17745 |
| Forest | 0 | 18552 | 770 | 35205 | 10877 | 7751 | 91774 | 5407 | 170336 |
| Water body | 0 | 4121 | 69 | 2483 | 222 | 1587 | 4950 | 23185 | 36616 |
| Total area in 2000 | 1833 | 62961 | 1528 | 67518 | 16896 | 21625 | 151868 | 35768 | 359997 |
| Total change | 0 | 23071 | −3099 | −8677 | 4142 | 3880 | −18468 | −848 | 0 |
| Percent (%) | 0 | 57.8 | −67.0 | −11.4 | 32.5 | 21.9 | −10.8 | −2.3 | 0 |

[a)]The land use types in the column and row represent those in 1990 and 2000, respectively. The data represent the land use/cover changes among various land types during the period 1990 to 2000.
[b)]UC = unclassified; HF = horticulture farm.

TABLE IV

Average land surface temperatures (means ± standard deviation) for various land cover types in the Zhujiang Delta in 1990 and 2000

| Land cover | 1990 | 2000 |
|---|---|---|
| | °C | |
| Urban or built-up land | 28.38 ± 2.917 | 32.94 ± 4.323 |
| Barren land | 26.84 ± 2.234 | 31.47 ± 4.918 |
| Cropland | 22.51 ± 1.584 | 27.67 ± 3.371 |
| Horticulture farms | 21.75 ± 1.392 | 24.93 ± 1.825 |
| Dike-pond land | 24.68 ± 2.621 | 28.00 ± 4.342 |
| Forest | 23.11 ± 2.063 | 25.67 ± 3.062 |
| Water body | 23.21 ± 3.411 | 24.59 ± 4.394 |

and concrete, did have an effect on raising LST.

The lowest LST in 1990 was observed in horticulture farms, followed by cropland, forest, water body, and dike-pond land. The pattern in 2000 was slightly different, where the lowest LST was found in water body, followed by horticulture farm, forest, cropland, and dike-pond land, probably due to the discrepancy in solar illumination, atmospheric influences, and soil moisture content in the two study years.

The LST for water body in 1990 was 0.10 °C higher than forest, a probable indication of the increasingly serious water pollution in the Zhujiang Delta, where wastewater from sugar refining, paper pulp processing, textile dyeing, and electroplating was often directly released into rivers without treatment. On the contrary, because dense orchards helped to reduce heat stored in the soil and surface structures through the transpiration process, horticulture farms showed a considerably low LST in both years. Similarly, horticulture farms demonstrated a relatively small standard deviation in LST (Table IV) compared with other land cover types. Because cropland, forest, and dike-pond land tended to have various portions of vegetation coverage and exposure of bare soil, they also had slightly different LST values with the influence imposed by vegetation transpiration and soil moisture content.

Profound impact of urban expansion on the modification of LST in the region was assessed through further investigation of the relationship between change of land use/cover types and that of LST. Image differencing operations were employed to produce an image of LST changes after the LST of each year was

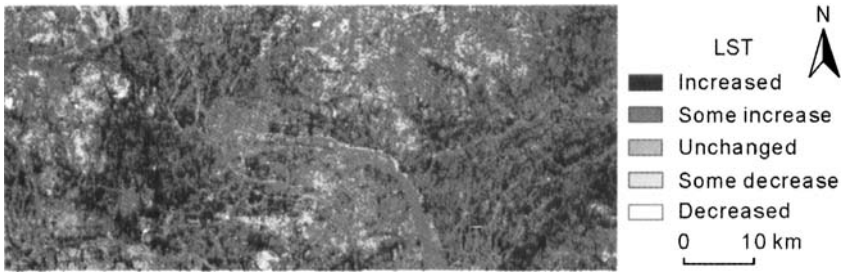


Fig. 1 The map of the land surface temperature (LST) change in the Zhujiang Delta from 1990 to 2000.

normalized (Fig. 1). This image was then overlaid with the image of urban expansion to obtain the change of LST in the newly urbanized region area. The results showed that urban development between 1990 and 2000 gave rise to an average of 4.56 °C in LST in these areas.

Pearson's correlation coefficients of LST in 1990 and 2000 were negatively correlated with NDVI for all land cover types in both years (Table V).

TABLE V

Pearson's correlation coefficients between average land surface temperature and normalized difference vegetation index for various land cover types

| Land cover | 1990 | 2000 |
|---|---|---|
| Urban or built-up land | −0.7251* | −0.8963* |
| Barren land | −0.4681* | −0.4778* |
| Cropland | −0.6121* | −0.6593* |
| Horticulture farms | −0.7016* | −0.8537* |
| Dike-pond land | −0.2928* | −0.3224* |
| Forest | −0.7685* | −0.8016* |
| Water body | −0.1857* | −0.1489* |

*Significant at $P = 0.05$.

This significant negative correlation between LST and NDVI implied that the higher biomass a land cover had, the lower its LST was. This relationship has determined that due to the associated changes in NDVI, changes in land use/cover would have an indirect impact on land surface temperatures. Fig. 2 showed that most pixels had a scaled NDVI value (*i.e.* $P_v$) less than zero generally indicating the reduced vegetation coverage from 1990 to 2000. For newly urbanized areas, the scaled NDVI decreased by 0.13 from 1990 to 2000.

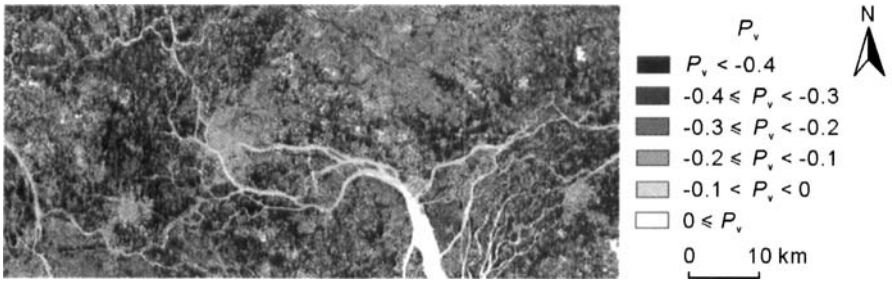


Fig. 2 The difference image for the scaled normalized difference vegetation index (NDVI), *i.e.* the fractional coefficient of vegetation coverage ($P_v$), in the Zhujiang Delta from 1990 to 2000.

The effect of LUCC on LST can also be visually examined using GIS. The LST change image obtained by image differencing was recoded into six temperature zones based on the equal interval classification scheme (Fig. 3). The area of each classification zone is summarized in Table VI, which

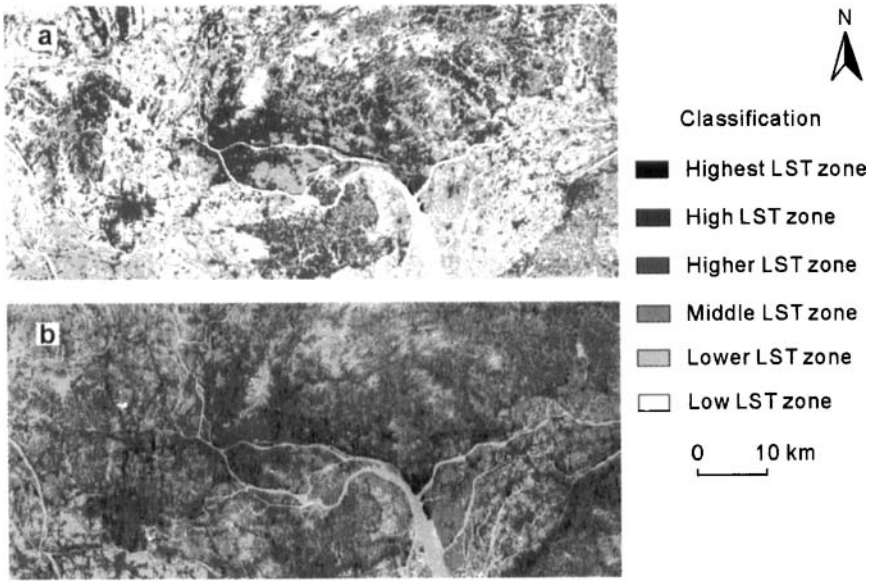


Fig. 3 Standard classification maps of land surface temperature (LST) for the Zhujiang Delta in 1990 (a) and 2000 (b).

TABLE VI

Standard classification areas based on the land surface temperature (LST) for the Zhujiang Delta in 1990 and 2000

| Classification | Code | Area | | | $I^{a)}$ |
|---|---|---|---|---|---|
| | | 1990 | 2000 | Change | |
| | | ha | | | |
| Low LST zone | 1 | 119774 | 2032 | −117742 | $0 < I \leq 0.2381$ |
| Lower LST zone | 2 | 117039 | 58976 | −58063 | $0.2381 < I \leq 0.3333$ |
| Middle LST zone | 3 | 56120 | 132731 | 76611 | $0.3333 < I \leq 0.4286$ |
| Higher LST zone | 4 | 64735 | 133448 | 68713 | $0.4286 < I \leq 0.5714$ |
| High LST zone | 5 | 1203 | 26654 | 25451 | $0.5714 < I \leq 0.7143$ |
| Highest LST zone | 6 | 413 | 6048 | 5635 | $I > 0.7143$ |
| Not classified | | 716 | 111 | −605 | $I = 0$ |

[a)] $I$ = index of classification.

shows that zones 3 to 6 have positive temperature changes (*i.e.* a temperature increase from 1990 to 2000), whereas zones 1 and 2 are negative. The classification map showed that the temperature change exhibited distinctly different spatial patterns among the six temperature zones. A detailed examination of these spatial patterns revealed that LST of zones 4 to 6 coincided with areas of urban expansion implying that urban expansion was primarily contributing to the increase in LST.

## CONCLUSIONS

The LUCC between 1990 and 2000 in the Zhujiang Delta revealed a notable change in land use/cover with an especially prominent increase of urban area. Examination of the relationship between LUCC (especially urban expansion) and the modification in LST showed that the change of land use/cover types caused a spatial redistribution of LST with LST raised 4.56 °C in newly developed urban areas. This demonstrated that the decrease of biomass primarily triggered the impacts of urban expansion on LST. The application of remote sensing and GIS proved to be an efficient way to detect LUCC and to evaluate its effect on LST. It provided not only detailed information on the nature, rate, and location of urban expansion but also the accompanying change of biophysical measurements, such as LST and biomass. This made it possible to investigate the impacts of human activities on the environment as

done in this study.

## REFERENCES


Balling, R. C. Jr. and Brazell, S. W. 1988. High resolution surface temperature patterns in a complex urban terrain. *Photogrammetric Engineering and Remote Sensing.* **54**: 1 289–1 293.

Gallo, K. P., McNab, A. L., Karl, T. R., Brown, J. F., Hood, J. J. and Tarpley, J. D. 1993. The use of NOAA AVHRR data for assessment of the urban heat island effect. *Journal of Applied Meteorology.* **32**(5): 899–908.

Gao, X. J., Luo, Y., Lin, W. T., Zhao, Z. C. and Giorgi, F. 2003. Simulation of effects of land use change on climate in China by a regional climate model. *Advances in Atmospheric Sciences.* **20**(4): 583–592.

Hu, X. F., Wu, H. X., Hu, X., Fang, S. Q. and Wu, C. J. 2004. Impact of urbanization on Shanghai's soil environmental quality. *Pedosphere.* **14**(2): 151–158.

Hurtado, E., Vidal, A. and Caselles, V. 1996. Comparison of two atmospheric correction methods for Landsat TM thermal band. *International Journal of Remote Sensing.* **17**(2): 237–247.

Kidder, S. Q. and Wu, H. T. 1987. A multispectral study of the St. Louis area under snow-covered conditions using NOAA-7 AVHRR data. *Remote Sensing of Environment.* **22**(2): 159–172.

Lo, C. P. 1989. Recent spatial restructuring in Zhujiang Delta, South China: A study of socialist regional development strategy. *Annals of the Association of the American Geographers.* **79**(2): 293–308.

Mansor, S. B., Cracknell, A. P., Shilin, B. V. and Gornyi, V. I. 1994. Monitoring of underground coal fires using thermal infrared data. *International Journal of Remote Sensing.* **15**(8): 1 675–1 685.

Oke, T. R. 1982. The energetic basis of the urban heat island. *Quarterly Journal of the Royal Meteorological Society.* **108**(455): 1–24.

Oppenheimer, C. 1997. Remote sensing of the colour and temperature of volcanic lakes. *International Journal of Remote Sensing.* **18**(1): 5–37.

Owen, T. W., Carlson, T. N. and Gillies, R. R. 1998. An assessment of satellite remotely-sensed land cover parameters in quantitatively describing the climatic effect of urbanization. *International Journal of Remote Sensing.* **19**(9): 1 663–1 681.

Pan, X. Z. and Zhao, Q. G. 2005. Monitoring and modeling of urban spatial expansion in Taihu Lake area, China in the last 50 years. I. A case study of Yixing City on monitoring of urban expansion. *Acta Pedologica Sinica* (in Chinese). **42**(2): 194–198.

Qin, Z. H. and Karnieli, A. 2001. A mono-window algorithm for retrieving land surface temperature from Landsat TM data and its application to the Israel-Egypt border region. *International Journal of Remote Sensing.* **22**(18): 3 719–3 746.

Qin, Z. H., Li, W. J., Zhang, M. H., Karnieli, A. and Berliner, P. 2003. Estimating of the essential atmospheric parameters of mono-window algorithm for land surface temperature retrieval from Landsat TM6. *Remote Sensing for Land & Resources* (in Chinese). (2): 37–43.

Qin, Z. H., Zhang, M. H., Karnieli, A. and Berliner, P. 2001. Mono-window algorithm for retrieving land surface temperature from Landsat TM6 data. *Acta Geographica Sinica* (in Chinese). **56**(4): 456–466.

Ritchie, J. C., Cooper, C. M. and Schiebe, F. R. 1990. The relationship of MSS and TM digital data with suspended sediments, chlorophyll, and temperature in Moon Lake, Mississippi. *Remote Sensing of Environment.* **33**(2): 137–148.

Roth, M., Oke, T. R. and Emery, W. J. 1989. Satellite derived urban heat islands from three coastal cities and the utilization of such data in urban climatology. *International Journal of Remote Sensing.* **10**(8): 1 699–1 720.

Saraf, A. K., Prakash, A., Sengupta, S. and Gupta, R. P. 1995. Landsat TM data for estimating ground temperature and depth of subsurface coal fire in Jharia coal field, India. *International Journal of Remote Sensing.* **16**(11): 2 111–2 124.

Sospedra, F., Caselles, V. and Valor, E. 1998. Effective wavenumber for thermal infrared bands application to Landsat TM. *International Journal of Remote Sensing.* **19**(11): 2 105–2 117.

Weng, Q. 1998. Local impacts of the post-Mao development strategy: The case of the Zhujiang Delta, southern China. *International Journal of Urban and Regional Studies.* **22**: 425–442.

Wu, L. X., Sun, B., Zhou, S. L., Huang, S. E. and Zhao, Q. G. 2004. A new fusion technique of remote sensing images for land use/cover. *Pedosphere.* **14**(2): 187–194.

Zhang, X., van Genderen, J. L. and Kroonenberg, S. B. 1997. A method to evaluate the capability of Landsat-5 TM band 6 data for sub-pixel coal fire detection. *International Journal of Remote Sensing.* **18**: 3 279–3 288.

Zhou, Q. X. 2006. Advance in the effects of climate change on environment and health. *Journal of Meteorology and Environment* (in Chinese). **22**(1): 38–44.

Zhou, W. M., Wang, J. D., Liu, J. S. and Yang, J. S. 2005. Influence of different land-use to regional climate in Sanjiang Plain. *Journal of Soil and Water Conservation* (in Chinese). **19**(5): 155–158.